Integrated Ferroelectrics, 123:32–39, 2011

ISSN: 1058-4587 print / 1607-8489 online
DOI: 10.1080/10584587.2011.570600

Taylor & Francis
Taylor & Francis Group

Numerical Evidences of Polarization Switching in PMN Type Relaxor Ferroelectrics

E. KLOTINS,[1] A. I. POPOV,[1] V. PANKRATOV,[1] L. SHIRMANE,[1] AND D. ENGERS[2,*]

[1]Institute of Solid State Physics, University of Latvia, 8 Kengaraga Str., Riga, LV-1063, Latvia
[2]Faculty of Physics and Mathematics, University of Latvia, 8 Zellu Str., Riga, LV-1002, Latvia

We present a conceptual and computational framework for chemically ordered $Pb(Mg_{1/3}Nb_{2/3}O_3)$ (PMN) type supercells violating disorder of the host lattice. The effective Hamiltonian is specified by invariance under permutations of supercells and by the dipole-dipole interaction supporting both local nonzero and zero mean polarization of the structure. Statistics treated in canonical ensemble within the mean field approach reveals emergence of polar nanoregions as supported by interplay between the (random) initial state polarization of supercells and their interactions increased at cooling.

Keywords Relaxor ferroelectrics; supercells; polar nano regions

1. Introduction

Extensive efforts to find unambiguous answer to what distinguishes relaxors from conventional freroelectrics have persisted since the 1983 [1] and are still an active field of research in condensed state theory. While ferroelectricity was originally conceived as a deviation of ions from its high symmetry positions the origin of relaxor properties was sought in replacing the translational invariance by compositional disorder. Presumably the disorder is supported by some atoms that might occupy randomly distributed off-center positions over the elementary cells as well as by quenched random fields resulting in the suppression of ferroelectric phase instability [2]. Abundant evidences of polar nanoregions found by the optic index of refraction [1], x-ray and neutron scattering [3, 4], piezoresponse force microscopy [5] as well as frequency dependence of the dielectric constant are systematized in [6, 7]. Despite spectacular success in phenomenological characterization of relaxors attempted within superparaelectric [8], dipolar glass [9] and local electric field [2] models the conceptual disadvantage is that local ordering emerges as a drastic contrast with the presumably disordered host lattice.

Recent developments in microscopic theory originates within the framework of effective (phonon) Hamiltonians fully specified by ab initio total-energy calculations for conventional ferroelectrics and resulting an accurate partition function for subsequent ab initio statistics [10, 11] as advancement. However, spatial invariance, implemented in this

Received May 25, 2010; in final form July 1, 2010.
*Corresponding author. E-mail: klotins@cfi.lu.lv

approach, is unreasonable for models of relaxors and leads to the model Hamiltonians phenomenologically augmented by random fields of defects [6, 12]. It is clearly important to look at the basis of aforementioned analysis and examine rigorously actual problems which arise for PMN type relaxor ferroelectrics, definitely, how to go round the presumption of off center ions and how to categorize the system in locally polar and locally nonpolar regions. In this study we report on construction of a mathematical model of $Pb(Mg_{1/3}Nb_{2/3}O_3)$ (PMN) from the standpoint of first principles lattice dynamics of chemically ordered supercells [13] violating the overall compositional disorder in B-sites. It allows us to quantify and explain the polarization switching of individual supercells as a candidate for assembling of the supercells in polar nano regions. Ingredients borrowed from the first principles lattice dynamics [13] include supercell lattice parameters whereas the thermodynamical arguments are restricted by invariance under permutations of ordered sites and zero spontaneous polarization of disordered sites. We give details of an effective Hamiltonian and mean field statistics simulations revealing the polarization switching and the assembling of suppercells as a prerequisite of polar nano regions.

The paper is organized as follows. Section 2 describes the effective Hamiltonians as derived from the polarization of structurally stable states [13], phenomenologically augmented for a simulation box of $8 \times 8 \times 8$ 15-ion supercells. The statistics of polarization switching of supercells and fingerprints of their assembling in polar nanoregions at cooling are found Sect. 3. Summary is in Sect. 4.

2. Effective Hamiltonians: Conceptual Setting and Approximations

The conceptual starting point is stoichiometry of $Pb(Mg_{1/3}Nb_{2/3}O_3)$ requiring at least one $Pb^{2+}Nb^{5+}O_3^{2-}$ and two $Pb^{2+}Mg^{2+}O_3^{2-}$ primitive lattice cells constituting an ordered 15 – ion supercell. A periodic array of ordered supercells [13, 14] with local 1:2 ordering along the [111] direction exhibit antiferroelectric, $P\bar{3}m1$, reference configuration unstable with respect to lover energy structurally stable ferroelectric state, $P1$, as found with the ab initio simulation package VASP. However, implications of supercells and its structural relaxation is certainly not complete to obtain first principles effective Hamiltonians [10, 15, 16] well accepted for statistical estimates in conventional ferroelectrics based on the Tailor expansion of potential energy and composed of the localized soft-mode amplitudes, their harmonic interactions and the strain.

A justified alternative then is to go around the local mode approach and exploit the properties of supercell in a periodic lattice as ingredients of the effective Hamiltonian. Then, we have supercell lattice parameters as: $a = 5.682, b = 5.759, c = 6.964, \alpha = 89.97$, $\beta = 90.48, \gamma = 120.43, \Omega_{cell} = 1.15742.10^{-28}$ (m^3) and ground state polarization as $P_x = 0.474$, $P_y = 0.476$, $P_z = 0.016$ (Cm^{-2}) (in Cartesian coordinate frame). Consequently, the effective Hamiltonian for a bare i-th supercell is given by low order Tailor expansion of potential energy with linear, λ, harmonic, α, and anharmonic, β terms

$$H_i^{loc} = -\frac{\alpha_x P_x^2}{2} - \frac{\alpha_y P_y^2}{2} - \frac{\alpha_z P_z^2}{2} + \frac{\beta_x P_x^4}{24} + \frac{\beta_y P_y^4}{24} + \frac{\beta_z P_z^4}{24} - \lambda \cdot \mathbf{P} \qquad (1)$$

The coefficients α, β, λ are found from (i) minimum energy constraint $\partial H_{ss1}/\partial P_\alpha = 0$ and (ii) the metastability excluded by setting the discriminant of minimum energy relation positive as $-8\alpha_\alpha^3 + 9\beta_\alpha\lambda_\alpha^2 = \varepsilon\beta_\alpha^3$, ($\alpha = x, y, z$ are Cartesian coordinates and ε is an infinitesimal positive constant). The third constraint is based on the energy of the supercell

$E_b = |\mathbf{P}|^2\,\Omega_{cell}\,(2\varepsilon_\infty\varepsilon_0)^{-1}$ that (on physical grounds) must be commensurable with thermal energy $E_t = k_B T$. At Burns temperature, $T_B \approx 650$(K), the condition $E_t = E_B$ gives estimate for the factor between the energy assigned to a bare supercell and its polarization square as $C_c = \Omega_{cell}\,(2\varepsilon\varepsilon_0)^{-1} = 1.98 \cdot 10^{-20}$ (m^4 V/C). Finally, the third constraint is determined by the energy of particular components of polarization as $-\frac{\alpha_\alpha P_\alpha^2}{2} + \frac{\beta_\alpha P_\alpha^4}{24} - \lambda_\alpha P_\alpha = -C_c P_\alpha^2$ and P_α are first principles results [13]. The corresponding energy landscape is distinguished by single well minima corresponding to the ground state polarization. Prepositions about the arrangement of supercells are as follows: (i) total energy involves invariance under permutations of the supercells, (ii) double degenerate states for supercells are reproduced by symmetric Miller indices, (iii) supercells with symmetric indices exhibit opposite polarization, and (iv) in a lattice of supercells the polarization is pseudorandom with zero mean for each component. Simulation box of $8\times8\times8$ supercells is specified by Cartesian coordinates $\{x_i, y_i, z_i\}$ for $i = 1, 2, ...8^3$ supercells and eight varieties of supercell polarization (triplets), $[\bar{1}\bar{1}\bar{1}]$, $[\bar{1}\bar{1}1]$, $[\bar{1}1\bar{1}]$, $[\bar{1}11]$,, $[1\bar{1}\bar{1}]$, $[1\bar{1}1]$, $[11\bar{1}]$, [111], with symmetric Miller indices, pseudorandom distribution of polarization and with zero mean for each component. The selection rule for invariance under permutations of supercells gives initial conditions for the temperature behavior and provides zero total polarization of the simulating box in accord with the disordered intrinsic structure of relaxors. Considering the simulation box as a heterogeneous system, the anisotropic dipole-dipole interaction between supercells is given by

$$H_i^{dpl} = \left[\frac{1}{2}\left(\frac{1}{4\pi\,\varepsilon_0}\right)\frac{1}{\varepsilon_\infty}\frac{\Omega_{cell}^2}{S_{cell}^3}\right]\sum_{j=1}^{j_{\max}}\frac{\mathbf{P}_i\cdot\mathbf{P}_j - 3(\mathbf{e}_{ij}\cdot\mathbf{P}_i)(\mathbf{e}_{ij}\cdot\mathbf{P}_j)}{R_{ij}^3} \tag{2}$$

Here $\mathbf{R}_i, \mathbf{R}_j$ are Cartesian coordinates of selected and interacting supercells, correspondingly. $R_{ij} = |\mathbf{R}_i - \mathbf{R}_j|$ is Euclidean distance between supercells and $\mathbf{e}_{ij} = \mathbf{R}_{ij}/|\mathbf{R}_{ij}|$ is the unit vector parallel to the line joining the centers of two supercells [10]. Estimates of supercell spacing $S_{cell} = 10^{-9}$ (m), optical dielectric constant of the host lattice, $\varepsilon_\infty = 10$ [6], constitutes the dipole-dipole interaction factor (the term in square brackets in Eq. (2)) as $6.011504 \cdot 10^{-21}$ ($\mathrm{Vm^4C^{-1}}$). The total Hamiltonian for i-th supercell is given by $H_i = H_i^{loc} + H_i^{dpl}$. The impact of the presumably disordered host lattice is hidden here in the supercell spacing, S_{cell}, as adjustable parameter.

3. Statistics of Supercells: Polarization Switching and Assembling

For the total Hamiltonian $H^{tot} = \sum_i (H_i^{loc} + H_i^{dip})$ the multivariate probability density involves statistics in canonical ensemble $\rho[\{\mathbf{P}_i;\mathbf{P}_j\}] \equiv \exp[-\beta H^{tot}]$. Here β is inverse temperature and the expectation value of polarization given by reads as

$$E(P_x) = \int P_x \rho(P_x, P_y, P_z) dP_y dP_z \tag{3}$$

and similar relations for $E(P_y)$,$E(P_z)$ [17]. Integration of Eqs. (3) started at high temperatures is preceded within the mean field approach, definitely, the unknown polarization $\mathbf{P}_j$ is replaced by the corresponding values of the initial conditions or, subsequently, by the values found over the preceding temperature step. Consequently, the impact of H^{dpl} contributes in local terms supplementary to the linearly terms in H^{loc}. Zero boundary conditions apply in this work.

Within the framework of this mean field approach the temperature is sequentially decreased, step by step, from above Burns temperature ($\approx$ 650 K [1, 9],) estimated as high enough to ignore the dipole-dipole interaction. At each temperature step, the polarization obtained from the previous iteration is used as the starting point for the next one including impact of the instant dipole-dipole interaction so cooling the system down to 10 K. What is expected from neutron diffuse scattering [4] is appearance of field-induced ferroelectric state at 210–220 K at cooling or, in terms of the supercell approach, supercell assembling is expected if going down the temperature scale. However, assembling of anisotropic supercells is available only as a result of polarization switching of individual supercells along a preferential direction. Temperature development of supercell # 220 with Cartesian coordinates {4, 4, 4} (in units of supercell spacing) belonging to the triplet of Miller indices $[\bar{1}, \bar{1}, 1]$ is illustrated in Fig. 1.

At high temperatures the expectation value of polarization Eq. (3) approaches to zero and so is the impact of dipole-dipole interaction. As a result the high temperature initial state belongs to the same triplet of Miller indices $[\bar{1}, \bar{1}, 1]$. If going down the temperature scale, the polarization of all supercells increases toward the minimum energy state. However, if the impact of dipole-dipole interaction Eq. (2) exceeds the linear term $\lambda \cdot \mathbf{P}$ in Eq. (1), the corresponding component of polarization changes its sign as illustrated in Fig. 1. Similar behavior is evidenced for all supercells in the simulation box as illustrated in Figs. 2 and 3 for components P_x and P_y.

What is expected and numerically evidenced at high temperatures is the number of aligned triplets (differentiated by its scalar product) close at 64 (within approximations in numerical integration in Eq. (3)). This balance is unavoidable violated at polarization switching of individual supercells and assembling of the supercells in polar nano regions as demonstrated in Figs. 4 and 5.

As demonstrated in Figs. 4 and 5 the number of supercells having aligned first neighbors enlarges at cooling as a fingerprint of their assembling in polar nanoregions. We find that these properties hold for a broad range of parameters.

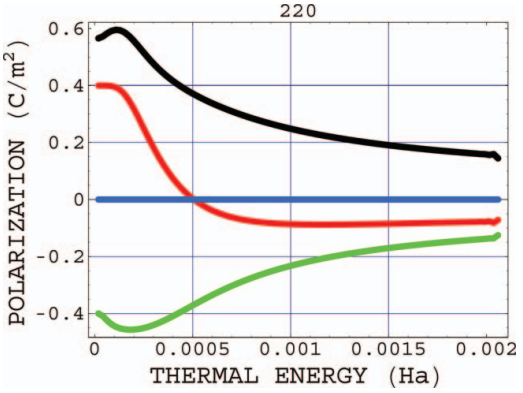

Figure 1. Temperature development of polarization for supercell #220 at cooling with P_x (green), P_y (red), P_z (blue) and $|\mathbf{P}|$ (black) plots. Numerical evidence of polarization switching which appear at thermal energy 0.0005 Ha (0.0005 Ha = 158 K) is assigned to the balance between the dipole-dipole interaction Eq. (2) and the impact of the linear term $\lambda_y P_y$ in Eq. (1).

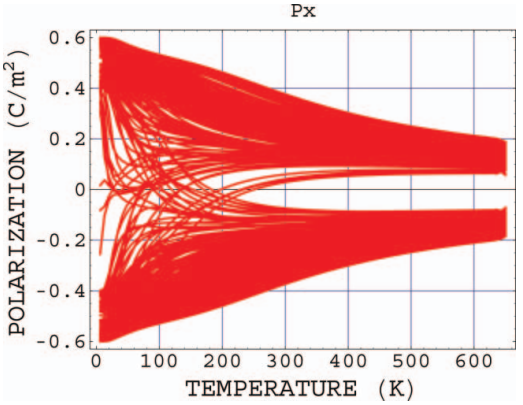

Figure 2. Temperature development of polarization P_x for all supercells in simulation box. At high temperature the initial polarization of each supercell approaches to zero maintaining the number of supercells belonging to one of the eighth available triplets. At cooling the polarization of individual supercells increases toward the minimum energy state or undergoes switching to the opposite sign, maintaining zero total polarization.

For the total Hamiltonian $H^{tot} = \sum_i (H_i^{loc} + H_i^{dip})$ the multivariate probability density involves statistics in canonical ensemble $\rho[\{\mathbf{P}_i; \mathbf{P}_j\}] \equiv \exp[-\beta H^{tot}]$. Here β is inverse temperature and the expectation value of polarization given by reads as

$$E(P_x) = \int P_x \rho(P_x, P_y, P_z) d P_y d P_z \tag{4}$$

and similar relations for $E\left(P_y\right), E\left(P_z\right)$ [17]. Integration of Eqs. (3) started at high temperatures is preceded within the mean field approach, definitely, the unknown polarization $\mathbf{P}_j$ is replaced by the corresponding values of the initial conditions or, subsequently, by the values found over the preceding temperature step. Consequently, the impact of H^{dpl} contributes

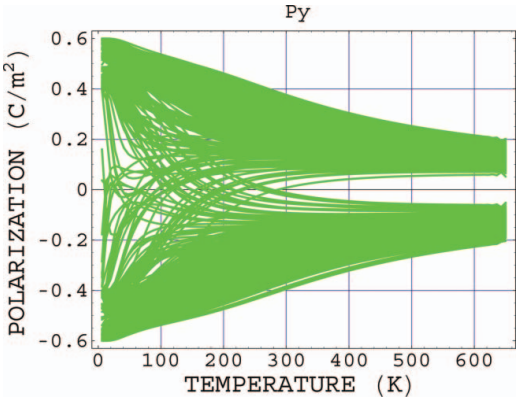

Figure 3. Temperature development of polarization P_y for all supercells in simulation box is similar to this of P_x.

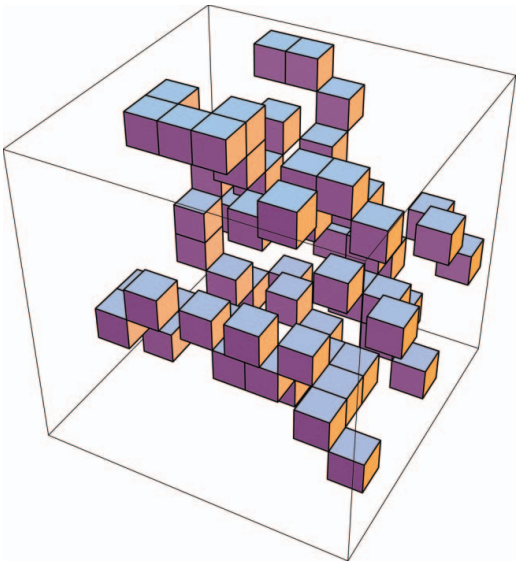

Figure 4. Supercell belonging to the $[\bar{1}, \bar{1}, 1]$ triplet at high temperature T = 650 K. Total number of aligned supercells 61.

in local terms supplementary to the linearly terms in H^{loc}. Zero boundary conditions apply in this work.

Within the framework of this mean field approach the temperature is sequentially decreased, step by step, from above Burns temperature ($\approx$ 650 K [9, 1]) estimated as high enough to ignore the dipole-dipole interaction. At each temperature step, the polarization

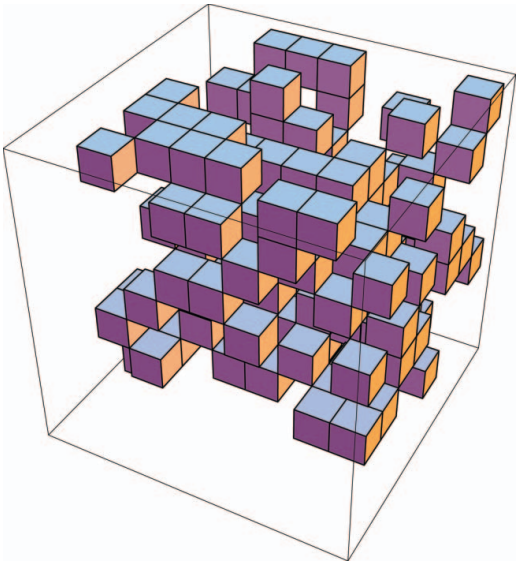

Figure 5. Supercell belonging to the $[\bar{1}, \bar{1}, 1]$ triplet at low temperature T = 6 K. Total number of aligned supercells 128 as a fingerprint of their assembling.

obtained from the previous iteration is used as the starting point for the next one including impact of the instant dipole-dipole interaction so cooling the system down to 10 K. What is expected from neutron diffuse scattering [4] is appearance of field-induced ferroelectric state at 210–220 K at cooling or, in terms of the supercell approach, supercell assembling is expected if going down the temperature scale. However, assembling of anisotropic supercells is available only as a result of polarization switching of individual supercells along a preferential direction.

Temperature development of supercell # 220 with Cartesian coordinates {4, 4, 4} (in units of supercell spacing) with Miller indices [$\bar{1}$, $\bar{1}$, 1] is illustrated in Fig. 1.

At high temperatures the expectation value of polarization Eq. (3) approaches to zero and so is the impact of dipole-dipole interaction. As a result the high temperature initial state belongs to the same triplet of Miller indices [$\bar{1}$, $\bar{1}$, 1]. If going down the temperature scale, the polarization of all supercells increases toward the minimum energy state. However, if the impact of dipole-dipole interaction Eq. (2) exceeds the linear term $\lambda \cdot \mathbf{P}$ in Eq. (1), the corresponding component of polarization changes its sign.

Similar behavior is evidenced for all supercells in the simulation box as illustrated in Figs. 2 and 3 for components P_x and P_y. What is expected and numerically evidenced at high temperatures is the number of aligned triplets (differentiated by its scalar product) close at 64 (within approximations in numerical integration in Eq. (3)). This balance in unavoidable violated at polarization switching of individual supercells and assembling of the supercells in polar nano regions as demonstrated in Figs. 4 and 5.

As demonstrated in Figs. 4 and 5 the number of supercells having aligned first neighbours enlarges at cooling as a fingerprint of their assembling in polar nanoregions. We find that these properties hold for a broad range of parameters.

4. Summary

We report construction of a mathematical model inspired by first principles lattice dynamics for chemically ordered supercells of PMN [13] phenomenologically augmented toward effective Hamiltonian. Characteristic features of this model are dipole-dipole interaction of the supercells and invariance under permutations as numerically evidenced preconditions of supercell assembling in polar nanoregions at cooling. While the stationary approach considered here neglects important effects of mode-mode interaction in supercells and the dynamics of the disordered host lattice, it suggests a framework within which to categorize the system in locally polar and locally nonpolar regions and rationalize the complex behaviour of PMN and related materials.

Acknowledgments

This work was supported by Latvian collaboration project # 05.0005

References

1. G. Burns and F. H. Dacol, Glassy polarization behavior in ferroelectric compounds $Pb(Mg_{1/3}Nb_{2/3})O_3$ and $Pb(Zn_{1/3}Nb_{2/3})O_3$. *Solid State Commun.* **48**, 853 (1983).
2. B. E. Vugmeister, Polarization dynamics and formation of polar nanoregions in relaxor ferroelectrics. *Phys. Rev. B* **73**, 174117 (2006).
3. K. Hirota, S. Waimoto, and D. E. Cox, Neutron and x-ray scattering studies of relaxors. *J. Phys. Soc. Jpn.* **75**, 111006 (2006).

4. P. M. Gehring, H. Hiraka, C. Stock, S.-H. Lee, W. Chen, Z.-G. Ye, S. B. Vahrushev, and Z. Chowdhury, Reassessment of the Burns temperature and its relationship to the diffuse scattering, lattice dynamics, and thermal expansion in relaxor $Pb(Mg_{1/3}Nb_{2/3})O_3$. *Phys. Rev. B* **79**, 224109 (2009).
5. V. V. Shvartsman and A. L. Kholklin, Domain structure of $0.8Pb(Mg_{1/3}Nb_{2/3})O_3$-$0.2PbTiO_3$ studied by piezoresponse force microscopy. *Phys. Rev. B* **69**, 014102 (2004).
6. B. P. Burton, E. Cockayne, S. Tinte, and U. V. Waghmare, First-principles-based simulations of relaxor ferroelectrics. *Phase Transitions*, **79**, pp. 91–121 (2006).
7. J. Macutkevic, S. Kamba, J. Banys, A. Brilingas, A. Pashkin, J. Petzelt, K. Bormanis, and A. Sternberg, Infrared and broadband dielectric spectroscopy of PZN-PMN-PSN relaxor ferroelectrics: Origin of two-component relaxation. *Phys. Rev. B* **74**, 104106 (2006).
8. L. E. Cross, "Relaxor Ferroelectrics", *Ferroelectrics* **76**, 241 (1987).
9. D. Vieland, J. Li, S. Jang, and L. E. Cross, Dipolar-glass model for lead magnesium niobate. *Phys. Rev. B* **43**, 8316 (1991).
10. W. Zong, D. Vanderbilt, and K. M. Rabe, Phase transitions in $BaTiO_3$ from first principles. *Phys. Rev. Lett.* **73**, 1861 (1994).
11. W. Zong, D. Vanderbilt, and K. M. Rabe, First-principles theory of ferroelectric phase transitions for perovskites: The case of $BaTiO_3$. *Phys. Rev. B.* **52**, 6301 (1995).
12. S. Tinte, B. P. Burton, E. Cockayne, and U. V. Waghmare, Origin of the relaxor state in $Pb(B_xB_{1-x'})O_3$ perovskites. *Phys. Rev. Lett.* **97**, 137601 (2006).
13. S. A. Prosandeev, E. Cockayne, B. P. Burton, S. Kamba, J. Petzelt, Yu. Yuzyuk, R. S. Katiyar, and S. B. Vakhrushev, Lattice dynamics in $PbMg_{1/3}Nb_{2/3}O_3$. *Phys. Rev. B* **70**, 134110 (2004).
14. N. Choudhury, Z. Wu, E. J. Walter, and R. E. Cohen, Ab initio linear response and frozen phonons for the relaxor $PbMg_{1/3}Nb_{2/3}O_3$. *Phys. Rev. B* **71**, 125134 (2005).
15. X. Zhao, D. Ceresoli, and D. Vanderbilt, Structural, electronic, and dielectric properties of amorphous ZrO2 from ab initio molecular dynamics. *Phys. Rev. B* **71**, 085107 (2005).
16. D. Fuks, S. Dorfman, S. Piskunov, and E. A. Kotomin, Ab initio thermodynamics of $Ba_cSr_{(1-c)}TiO_3$ solid solutions. *Phys. Rev B* **71**, 014111 (2005).
17. N. G. Van Kampen, Stochastic Processes in Physics and Chemistry, Fifth impression, (ELSEVIER, 2004).